Progress of Theoretical Physics, Vol. 87, No. 5, May 1992

Antisymmetrized Version of Molecular Dynamics with Two-Nucleon Collisions and Its Application to Heavy Ion Reactions

Akira ONO, Hisashi HORIUCHI, Toshiki MARUYAMA and Akira OHNISHI

Department of Physics, Kyoto University, Kyoto 606-01

(Received January 8, 1992)

Two-nucleon collision process is incorporated into the antisymmetrized version of the molecular dynamics by utilizing the technique and the concept developed in the time-dependent cluster model. This newly formulated method of microscopic simulation of the heavy ion reaction can describe quantum mechanical features such as shell effects, since it treats the time development of the system wave function. We also propose a new prescription by which we can avoid the spurious zero-point energies of center-of-mass motion of fragment wave packets. The fragment production cross sections of the $^{12}C+^{12}C$ reaction at 28.7 MeV/nucleon are analyzed by this new method. It is shown that the basic feature of the data including the large cross section of α-particle is reproduced well by the theory. Furthermore we show that the data are reproduced very well when we take into account the statistical cascade decays of the produced fragments, which verifies the great usefulness of the new microscopic simulation framework.

§ 1. Introduction

In heavy ion collisions, there appear various kinds of reaction mechanisms depending on the incident energy and on the impact parameter. Microscopic simulations of heavy ion reactions play an essential role for the understanding of these reaction mechanisms and transitions among them because they give us a unified theoretical framework for the description of heavy ion reactions. An important clue to characterize heavy ion reaction mechanisms is the fragments (or clusters) produced in various reaction processes; for example a large compound nucleus together with some small clusters and nucleons in the fusion reaction at low incident energy, and many small clusters and nucleons in the multi-fragmentation process at high incident energy. Among many microscopic simulation methods, the quantum molecular dynamics (QMD) by Aichelin and Stöcker,[1] which is considered to be an N-body theory, has been one of a few tractable approaches which can describe both the mean field effect and the dynamics of the fragment formation. QMD has been successfully applied not only to high energy heavy ion collisions but also to low and intermediate energy reactions including fusion reactions.[1~4]

In spite of these successes of QMD, its theoretical basis on quantum many body theory still needs to be made clearer. In QMD, nucleons are represented by distinguishable Gaussian wave packets in phase space. Due to this approximation, the ground states of nuclei, which are necessary as the initial states of simulations, are constructed only in a semi-classical way, for example by mimicking the phase space distribution of Thomas-Fermi model in order not to violate the Pauli principle requirement that each phase space unit with h^3 volume does not contain more than one nucleon. The time development of the centers of wave packets is determined by two processes; the propagation due to the classical equation of motion and the stochastic

two-nucleon collision process. In the latter process, fermionic nature of nucleons is taken into account by the Pauli blocking of final state. In the former process, on the other hand, nucleons are treated as if they are classical (or distinguishable) particles, but the Pauli principle in phase space occupancy is respected approximately in the sense that the propagation in QMD is an approximation of Vlasov dynamics[5)~8)] in which the Pauli principle is not violated due to the Liouville theorem of classical mechanics. (See Ref. 9) for discussions of this problem.) In order to have improved treatment of the fermionic nature of nucleons, many authors have introduced recently Pauli potentials into QMD.[10),11)] It should be noted here that when a Pauli potential is introduced into QMD, the QMD is essentially the same as the method of quasi-particle dynamics developed by Boal and his collaborators.[12)]

Recently, Feldmeier[13)] introduced the antisymmetrized version of molecular dynamics which he called fermionic molecular dynamics (FMD). In this framework the wave function of many body system is described by a Slater determinant of Gaussian wave packets of nucleons, and the time development of the parameters of wave packets is determined by time-dependent variational principle.[14)] The fermionic nature of nucleons is of course treated exactly in this method. Several groups have been studying this FMD framework.[15)~18)] Some of the present authors have used a restricted version of FMD by neglecting the time variation of the width parameters and that of the spin wave functions.[15),16)] By this restriction they have been able to treat many-nucleon systems and they have demonstrated that the antisymmetrized version of the molecular dynamics combined with the frictional cooling method[19)] is very powerful for the study of nuclear structure since this method is free from model assumptions such as the assumption of the axial symmetry and that of the clustering structure.

It is therefore hopeful that the antisymmetrized version of molecular dynamics can serve as an excellent simulation method for the heavy ion reaction. However in order to treat heavy ion collisions, it is indispensable to incorporate the two-nucleon collision process into this framework.

The present authors have succeeded in formulating a method to incorporate the two-nucleon collision process into the antisymmetrized version of the molecular dynamics. It means that they have constructed a new microscopic simulation framework which is an antisymmetrized version of the QMD. Hereafter in this paper we call this new simulation framework simply AMD. The purpose of this paper is twofold. One is to give a detailed explanation of this new method AMD and the other is to report an example of applications of the AMD to the study of fragment formation in heavy ion collisions.

Although we have introduced AMD as an antisymmetrized version of QMD, AMD is also interpreted as an extended version of time-dependent cluster model (TDCM).[20)~23)] If all clusters in the TDCM wave function are taken to be single nucleons, the TDCM wave function is the same as the AMD wave function. In fact, the treatment of two-nucleon collisions in AMD has been formulated by utilizing the technique and the concept developed in the TDCM. We construct physical nucleon coordinates as an extension of canonical coordinates in the case of two nucleons (or two clusters) derived by Saraceno et al.[22)] in the TDCM. Physical coordinates are

necessary because the centers of nucleon wave packets do not always have the meaning as the physical positions and momenta of nucleons due to the antisymmetrization effect and hence they cannot be used directly for the description of two-nucleon collision processes. There exists Pauli forbidden region in the phase space for the newly constructed physical nucleon coordinates, which is the same situation as in the TDCM.[22] The Pauli blocking in two-nucleon collisions in AMD is formulated so as to prohibit nucleons from entering into the Pauli forbidden region.

Since AMD is a framework which treats the time development of the wave function, it can describe quantum mechanical features such as shell effects. The ground states of colliding nuclei which constitute the initial states of simulation are now supplied in the form of the wave functions constructed with the frictional cooling method. As mentioned above these ground state wave functions describe the observed spectroscopic properties well which of course includes shell effects and clustering effects if any.[15),16] The ability of the AMD to treat shell effects is expected to play important roles also in the description of the dynamical formation process of fragments.

In any wave packet theory such as TDCM, QMD and the present AMD, there inevitably appears the problem of the zero-point kinetic energy of the nucleus or cluster. When the fragmentation of a nucleus into N_F fragments is described by a wave packet theory, the zero-point kinetic energy of the center-of-mass motion of each fragment, whose average value is denoted as T_0, may cause a serious trouble, because the effective value of the fragmentation threshold energy is higher than its real value by the amount of $(N_F-1)T_0$. We propose in this paper a phenomenological prescription by which we avoid this spurious energy effect, and we actually use it in our AMD study of the fragment formation in heavy ion collisions.

In order to verify the usefulness of the AMD, we have applied AMD for the study of the fragment formation in the heavy ion reaction. We report in this paper calculated results of the fragment mass distribution of the $^{12}C+^{12}C$ reaction at 28.7 MeV/nucleon which are compared with the data by Czudek et al.[25] The basic feature of the data will be seen to be reproduced by the calculation. We will notice that the calculated cross section of the α-particle production is very large and is comparable with the nucleon cross section. This result is quite different from the QMD calculation which does not show such a shell effect or α-clustering effect.

The fragments obtained in microscopic simulation calculations by the time of a few hundred fm/c after the first contact of colliding nuclei are usually not in their ground states but in highly excited states. Hence they should decay by evaporating particles during long time scale which microscopic simulation calculations cannot trace. Therefore we have made a calculation of statistical cascade decays of the excited fragments produced in the AMD calculation of the above-mentioned $^{12}C+^{12}C$ reaction. We will see that the fragment production cross sections obtained after the treatment of the statistical cascade decays reproduce the data very well. It is a strong verification of the great usefulness of the new simulation framework AMD.

This paper is organized as follows. In § 2, the AMD without inclusion of two-nucleon collisions is explained. Here we present and explain a prescription by which we avoid the spurious effect due to the zero-point center-of-mass energies of frag-

ments. In § 3, we explain how we treat the two-nucleon collision process in the AMD. We report in § 4 the results of the application of the AMD to the study of the fragment formation in $^{12}C+^{12}C$ reaction at 28.7 MeV/nucleon. Finally in § 5 we give a summary and discussion.

§ 2. AMD without two-nucleon collisions

2.1. *Equation of motion*

In AMD, the wave function of A-nucleon system $|\Phi\rangle$ is described by a Slater determinant,

$$|\Phi\rangle=\frac{1}{\sqrt{A!}}\det[\varphi_i(j)], \tag{2·1}$$

where

$$\varphi_i=\phi_{Z_i}\chi_{\alpha_i}. \tag{2·2}$$

α_i represents the spin and isospin of i-th single particle state, $\alpha_i=$p↑, p↓, n↑, or n↓, and χ is the spin and isospin wave function. ϕ_{Z_i} is the spatial wave function of i-th single particle state, which is a Gaussian,

$$\langle \boldsymbol{r}|\phi_{Z_i}\rangle=\left(\frac{2\nu}{\pi}\right)^{3/4}\exp\left[-\nu\left(\boldsymbol{r}-\frac{\boldsymbol{Z}_i}{\sqrt{\nu}}\right)^2+\frac{1}{2}\boldsymbol{Z}_i^2\right], \tag{2·3}$$

where ν is a parameter which represents the width of the wave packet. Note that $|\phi_Z\rangle$ is the coherent state of harmonic oscillator,

$$\boldsymbol{a}|\phi_Z\rangle=\boldsymbol{Z}|\phi_Z\rangle, \tag{2·4}$$

$$\boldsymbol{a}\equiv\sqrt{\nu}\,\boldsymbol{r}+\frac{i}{2\hbar\sqrt{\nu}}\boldsymbol{p}, \tag{2·5}$$

and if we define $\boldsymbol{D}$ and $\boldsymbol{K}$ as

$$\boldsymbol{Z}=\sqrt{\nu}\,\boldsymbol{D}+\frac{i}{2\hbar\sqrt{\nu}}\boldsymbol{K}, \tag{2·6}$$

then

$$\frac{\langle\phi_Z|\boldsymbol{r}|\phi_Z\rangle}{\langle\phi_Z|\phi_Z\rangle}=\boldsymbol{D},\quad \frac{\langle\phi_Z|\boldsymbol{p}|\phi_Z\rangle}{\langle\phi_Z|\phi_Z\rangle}=\boldsymbol{K}. \tag{2·7}$$

But due to the effect of antisymmetrization, $\boldsymbol{D}_i$ and $\boldsymbol{K}_i$ cannot always be interpreted as physical positions and momenta of nucleons, as can be seen in the following sections. These single particle states are not mutually orthogonal and their overlaps are

$$B_{ij}\equiv\langle\varphi_i|\varphi_j\rangle=e^{\boldsymbol{Z}_i^*\cdot\boldsymbol{Z}_j}\delta_{\alpha_i\alpha_j}, \tag{2·8}$$

and the norm of $|\Phi\rangle=|\Phi(\boldsymbol{Z})\rangle$ is

$$\mathcal{N}(\boldsymbol{Z}, \boldsymbol{Z}^*)=\langle \Phi(\boldsymbol{Z})|\Phi(\boldsymbol{Z})\rangle=\det B\,. \tag{2·9}$$

Thus A-body wave function $|\Phi\rangle$ is parametrized by the centers of Gaussians $\{\boldsymbol{Z}\}=\{\boldsymbol{Z}_i(i=1, 2, \cdots, A)\}$, and their time developments are determined by the time-dependent variational principle,

$$\delta\int_{t_1}^{t_2} dt \frac{\langle \Phi(\boldsymbol{Z})|\left(i\hbar\frac{d}{dt}-H\right)|\Phi(\boldsymbol{Z})\rangle}{\langle \Phi(\boldsymbol{Z})|\Phi(\boldsymbol{Z})\rangle}=0 \tag{2·10}$$

with the condition

$$\delta\boldsymbol{Z}(t_1)=\delta\boldsymbol{Z}^*(t_1)=\delta\boldsymbol{Z}(t_2)=\delta\boldsymbol{Z}^*(t_2)=0\,. \tag{2·11}$$

This equation leads to the equation of motion for $\{\boldsymbol{Z}\}$,

$$i\hbar\sum_{j\tau} C_{i\sigma,j\tau}\dot{Z}_{j\tau}=\frac{\partial\mathcal{H}}{\partial Z^*_{i\sigma}} \quad \text{and c.c.,} \tag{2·12}$$

where $\sigma, \tau=x, y, z$. $\mathcal{H}$ is the expectation value $\langle H\rangle$ of Hamiltonian H,

$$\mathcal{H}(\boldsymbol{Z}, \boldsymbol{Z}^*)=\frac{\langle \Phi(\boldsymbol{Z})|H|\Phi(\boldsymbol{Z})\rangle}{\langle \Phi(\boldsymbol{Z})|\Phi(\boldsymbol{Z})\rangle} \tag{2·13}$$

and

$$\begin{aligned} C_{i\sigma,j\tau}&=\frac{\partial^2}{\partial Z^*_{i\sigma}\partial Z_{j\tau}}\log\mathcal{N} \\ &=(\delta_{\sigma\tau}+Z^*_{i\tau}Z_{j\sigma})B_{ij}B^{-1}_{ji}-\sum_{kl}Z^*_{k\tau}Z_{l\sigma}B_{il}B^{-1}_{lk}B_{kj}B^{-1}_{ji} \end{aligned} \tag{2·14}$$

is a positive definite hermitian matrix.

$C_{i\sigma,j\tau}$ is covariant under rotation because B_{ij} is invariant as is evident from Eq. (2·8). Under Galilei transformation, $B_{ij}B^{-1}_{ji}$ and $B_{il}B^{-1}_{lk}B_{kj}B^{-1}_{ji}$ in Eq. (2·14) are invariant because of the equation

$$\begin{aligned} \sum_h\frac{\partial}{\partial\boldsymbol{Z}^*_h}B_{ij}B^{-1}_{jk}&=\sum_h\frac{\partial B_{ij}}{\partial\boldsymbol{Z}^*_h}B^{-1}_{jk}-\sum_{hmn}B_{ij}B^{-1}_{jm}\frac{\partial B_{mn}}{\partial\boldsymbol{Z}^*_h}B^{-1}_{nk} \\ &=\boldsymbol{Z}_jB_{ij}B^{-1}_{jk}-\sum_{mn}B_{ij}B^{-1}_{jm}\boldsymbol{Z}_nB_{mn}B^{-1}_{nk} \\ &=0 \end{aligned} \tag{2·15}$$

and its complex conjugate equation

$$\sum_h\frac{\partial}{\partial\boldsymbol{Z}_h}B_{ji}B^{-1}_{kj}=0\,. \tag{2·16}$$

Using this fact, $C_{i\sigma,j\tau}$ is easily proved to be Galilei invariant. Since $\mathcal{H}$ is invariant under rotation and translation, the equation of motion (2·12) is covariant under rotation and invariant under translation, which leads to the conservation of total angular momentum and total momentum.

We solve the equation of motion (2·12) by Euler method, which is a kind of second order Runge-Kutta method, with the time step $\Delta t=0.75$ fm/c. $|\dot{\boldsymbol{Z}}_i-\dot{\boldsymbol{Z}}_j|$ sometimes

becomes very large because the matrix C in (2·12) can have very small eigenvalues when $\boldsymbol{Z}_i$ and $\boldsymbol{Z}_j$ are very close in phase space. In such situations, we modify the time step Δt so that $|\dot{\boldsymbol{Z}}_i-\dot{\boldsymbol{Z}}_j|\Delta t$ is not too large.

2.2. *Zero-point kinetic energy of fragments*

The expectation value of center-of-mass kinetic energy $T_{\rm CM}$ is given by

$$\langle T_{\rm CM}\rangle = T_0+\frac{1}{2AM}\boldsymbol{K}_{\rm CM}^2\,, \tag{2·17}$$

where

$$T_0=\frac{3\hbar^2\nu}{2M}\,, \tag{2·18}$$

$$\sum_{i=1}^{A}\boldsymbol{Z}_i=\sqrt{\nu}A\boldsymbol{D}_{\rm CM}+\frac{i}{2\hbar\sqrt{\nu}}\boldsymbol{K}_{\rm CM}\,. \tag{2·19}$$

T_0 is the kinetic energy due to the zero-point oscillation of center-of-mass motion, which appears because center-of-mass wave function is fixed to be a Gaussian wave packet in our model. This does not cause any trouble as long as we are interested in nuclear structure, since AMD wave function is factorized into the product of center-of-mass wave function and internal wave function, and there is no spurious coupling between them.

This unphysical center-of-mass zero-point kinetic energy, however, may cause a serious trouble in treating fragment formation. Let us consider, for example, the case of ^{12}C and 3α, assuming that binding energies of ^{12}C and α are reproduced in our model, i.e., $|\langle H\rangle_{^{12}\rm C}-T_0|=E_{^{12}\rm C}=92.2$ MeV and $|\langle H\rangle_\alpha-T_0|=E_\alpha=28.3$ MeV. In the physical situation, the energy necessary to break a ^{12}C into 3α is $E_{^{12}\rm C}-3E_\alpha=7.3$ MeV. In our model, the energy of ^{12}C ground state is $\langle H\rangle_{^{12}\rm C}=-E_{^{12}\rm C}+T_0$ and that of 3α state is $3\langle H\rangle_\alpha=3(-E_\alpha+T_0)$. The difference of them is therefore $E_{^{12}\rm C}-3E_\alpha+2T_0$. The extra term $2T_0$ appears because the wave functions of relative motions of 3α are fixed to be Gaussian wave packets of a given width parameter. In general, extra energy T_0 is necessary when the number of fragments increases by one. When we take $\nu=0.16$ fm^{-2}, $T_0=10.0$ MeV, which cannot be ignored.

Note that this trouble is not peculiar to AMD. It already exists in time-dependent Hartree-Fock theory as well as in all time-dependent wave packet theories.

In order to avoid this kind of trouble, it is better to supply this extra energy from outside, or in other words, to subtract zero-point oscillation energy of fragments from Hamiltonian in the equation of motion (2·12),

$$\mathcal{H}=\langle H\rangle-T_0N_{\rm F}\,. \tag{2·20}$$

$N_{\rm F}$ is the "number of fragments," which is a function of $\{\boldsymbol{D}\}=\{\boldsymbol{D}_i(i=1,2,\cdots,A)\}$, i.e., real parts of $\{\boldsymbol{Z}\}$. This should coincide with the true number of fragments for those configurations in which clustering can be identified without ambiguity, and $N_{\rm F}$ should connect these configurations smoothly. The term $-T_0N_{\rm F}$ is expected to act as a repulsive potential when a fragmentation occurs.

Next we will derive N_F as a continuous function of configuration $\{\boldsymbol{D}\}$. The simplest version of N_F can be written as

$$N_F^{(1)}=\sum_{i=1}^{A}\frac{1}{m_i^{(1)}}, \tag{2·21}$$

$$m_i^{(1)}=\sum_{j=1}^{A}f_{ij}, \tag{2·22}$$

where f_{ij} represents the "friendship" between nucleons i and j, i.e., f_{ij} is 1 if two nucleons i and j are in the same fragment, and 0 if they belong to different fragments. Between these extreme situations f_{ij} takes value between 0 and 1. $m_i^{(1)}$ defined by (2·22) is therefore the number of friends of nucleon i (including itself), which takes continuous value. It is easily understood that $N_F^{(1)}$ defined by (2·21) certainly gives the correct fragment number in the case of unambiguous clustering, because $m_i^{(1)}$ is equal to the mass number of the fragment that includes nucleon i. We assume that friendship f_{ij} can be replaced by a function of $d_{ij}=|\boldsymbol{D}_i-\boldsymbol{D}_j|$ such as

$$f_{ij}=f(d_{ij})=\begin{cases}1 & \text{if } d_{ij}\leq a,\\ e^{-\nu(d_{ij}-a)^2} & \text{if } d_{ij}>a,\end{cases} \tag{2·23}$$

where we take $a=0.5$ fm.

As an example and a check of our definition, let us consider the case in which A_1 nucleons are at the same point and remaining A_2 nucleons are at another point which is apart from the former nucleons by a distance d. These two clusters are called cluster 1 and cluster 2. The fragment number defined by (2·21) and (2·22) can be written as

$$N_F^{(1)}(d)=\frac{A_1}{A_1+A_2f(d)}+\frac{A_2}{A_2+A_1f(d)}. \tag{2·24}$$

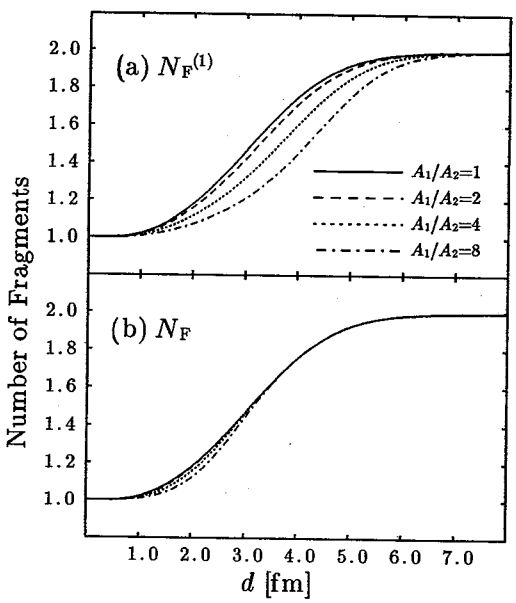

Fig. 1. (a) The simplest fragment number $N_F^{(1)}$ as a function of distance d between two clusters 1 and 2 for various mass ratio A_1/A_2.
(b) The modified version of fragment number N_F.

In Fig. 1(a), this is plotted for various mass ratio A_1/A_2. Although they have proper limits for $d\to 0$ and $d\to\infty$, they depend strongly on mass ratio. It is more difficult for a nucleon to go out from a heavy cluster than for a composite particle such as a deuteron or an alpha. Since this dependence is not desirable, we must modify the definition of N_F.

An easy way to avoid such mass ratio dependence is to replace the clusters 1 and 2 with two *nucleons* and then calculate the fragment number by (2·21)

and (2·22). In order to perform this modification for general configurations, we first count the number of "close friends" of nucleon i by friendship $\hat{f}_{ij}$ as

$$n_i=\sum_{j=1}^{A}\hat{f}_{ij}\,. \tag{2·25}$$

In the above example, it is ideal that $n_i=A_k$ when nucleon i belongs to the cluster k ($k=1, 2$). Then we attach a weight $1/n_i$ to each nucleon i instead of replacing each group which consists of close friends with a *nucleon*, and calculate the fragment number N_F in the same way as Eqs. (2·21) and (2·22),

$$N_F=\sum_{i=1}^{A}\frac{1}{n_i}\frac{1}{m_i}\,, \tag{2·26}$$

$$m_i=\sum_{j=1}^{A}\frac{1}{n_j}f_{ij}\,. \tag{2·27}$$

In a similar way to Eq. (2·23), $\hat{f}_{ij}$ is replaced by a function of $d_{ij}=|\boldsymbol{D}_i-\boldsymbol{D}_j|$. From the above consideration the judgement of friendship by $\hat{f}_{ij}$ should be stricter than that by f_{ij}. We therefore define as

$$\hat{f}_{ij}=\hat{f}(d_{ij})=\begin{cases}1 & \text{if } d_{ij}\leq\hat{a}\,,\\ e^{-2\nu(d_{ij}-\hat{a})^2} & \text{if } d_{ij}>\hat{a}\,,\end{cases} \tag{2·28}$$

where we take $\hat{a}=0.25$ fm. For the above example of two clusters, $N_F(d)$ is also parametrized by mass ratio A_1/A_2. In Fig. 1(b), $N_F(d)$ is shown for various mass ratio. As we have expected, the mass ratio dependence has been reduced considerably.

2.3. *Initialization*

The ground states of nuclei are constructed by frictional cooling method.[15),16)] We introduce an equation of motion which is given by multiplying a complex factor $\lambda+i\mu$, $\mu<0$, to the right-hand side of AMD equation of motion (2·12). It is easily proved that the energy decreases with time if the system follows this equation of motion. Starting with randomly chosen $\{\boldsymbol{Z}\}$ and solving this equation of motion, we reach the ground state of the nucleus.

We use Volkov No. 1 force[24)] as the effective interaction. Coulomb interaction is approximated by a sum of seven Gaussians. This approximation is valid for 1 fm $<r<$20 fm. The width parameter ν is chosen to be 0.16 fm^{-2}. In Eq. (2·20), T_0 was zero-point oscillation kinetic energy and therefore was equal to 10.0 MeV. But from now on, we treat T_0 as an adjustable parameter. $T_0=0$ corresponds to no subtraction of zero-point kinetic energy of fragments and $T_0=10.0$ MeV corresponds to the full subtraction. Energy is shifted by a constant so that the energy is zero when A nucleons of zero momenta exist separately,

$$\mathcal{H}=\langle H\rangle-\frac{3\hbar^2\nu}{2M}A+T_0(A-N_F)\,. \tag{2·29}$$

In order to reproduce binding energies of ^{12}C and α, we choose Majorana parameter

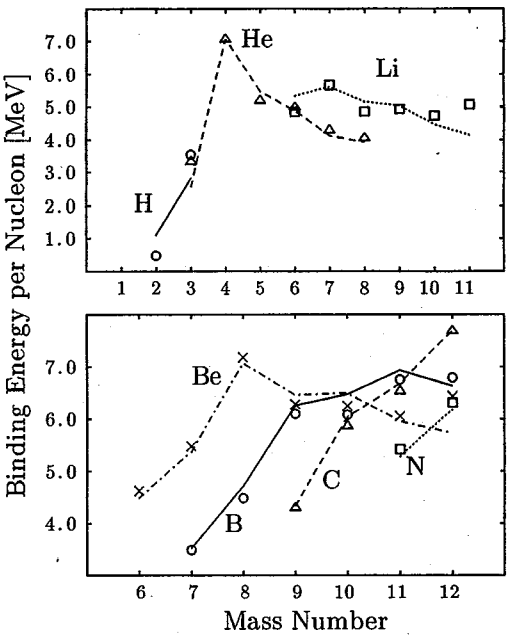

Fig. 2. Binding energies per nucleon of various nuclei. Points are the binding energies calculated by frictional cooling method and lines connect experimental values of the isotopes.

$m=0.576$ and $T_0=7.7$ MeV. In Fig. 2 binding energies of various nuclei of mass number $A\leq 12$ are shown. Binding energy is defined as $-\mathcal{H}$ at the ground state. The agreement with experimental value is wonderfully good. This is partly because AMD can describe the shell effect in the binding energies due to the antisymmetrization, and partly because we have one more free parameter T_0.

Binding energies, however, should not have been reproduced in principle, because we have not carried out the projection of parity and angular momentum and furthermore the width parameter ν is independent of nuclei. But we are interested in the effect of Q-values in heavy ion collisions, rather than the details of the structure of nuclei. It is therefore preferable that binding energies are reproduced in our model, even though the wave function is not perfectly described.

Because we are going to investigate the reaction $^{12}C+^{12}C$ in § 4, we will explain in some detail the ground state of ^{12}C which is constructed by frictional cooling method. Near the ground state of ^{12}C, all $\boldsymbol{Z}$ are almost equal to 0. Twelve $\boldsymbol{Z}$ are divided into three groups each of which consists of four $\boldsymbol{Z}$ of different spin and isospin. In each group, four $\boldsymbol{Z}$ have almost common value, but protons are slightly outer than neutrons due to the effect of Coulomb interaction. The limit that all $\boldsymbol{Z}$ are at the same point seems to be the minimum energy state. In this limit the wave function is the shell model wave function, $(0s)^4(0p)^8$. The energy of this minimum energy state is -92.2 MeV. Because this state is a singular point of our model, we use a slightly excited state as an initial state of simulations. This state is taken from the middle stage of the frictional cooling. The excitation energy of this state is 0.7 MeV, which seems negligible. The root mean square radius of this state is 2.49 fm, which agrees with the experimental value 2.48 fm. When this state is time-developed, the r.m.s. radius vibrates because the state is not the true ground state. But the amplitude of this oscillation is only 0.0015 fm. This state is time-developed for randomly chosen time and rotated randomly. Two initial nuclei prepared in this way are boosted toward each other on the Coulomb trajectory.

§ 3. Two-nucleon collisions

3.1. *Physical coordinates*

When we apply AMD to heavy ion reactions, it is indispensable to include two-nucleon collision processes. In quantum molecular dynamics (QMD), two nucleons are made to scatter stochastically when their spatial distance is small. As soon as we try to incorporate two-nucleon collisions into AMD in the same manner as QMD, we encounter a new problem as pointed out in Ref. 15). The centers of Gaussian wave packets $\{\boldsymbol{Z}\}$ do not always have the meaning as the positions and momenta of nucleons due to the effect of antisymmetrization. In the ground state of ^{12}C, for example, all $\boldsymbol{Z}$ are almost at the same point, but this does not mean that all nucleons are at the same point. We would like to have a QMD-like picture that nucleons which are represented by Gaussian wave packets are distributed without antisymmetrization effect. For this end, we have to transform coordinates $\{\boldsymbol{Z}\}$ to new coordinates $\{\boldsymbol{W}\}=\{\boldsymbol{W}_i(i=1, 2, \cdots, A)\}$ which can be interpreted as the centers of incoherent Gaussian wave packets. The real parts $\boldsymbol{R}_i$ and the imaginary parts $\boldsymbol{P}_i$ of $\boldsymbol{W}_i$,

$$\boldsymbol{W}_i=\sqrt{\nu}\,\boldsymbol{R}_i+\frac{i}{2\hbar\sqrt{\nu}}\boldsymbol{P}_i\,, \tag{3·1}$$

can be treated as physical positions and momenta of nucleons in the two-nucleon collision processes.

We have the following requirements which should be satisfied by physical coordinates $\{\boldsymbol{W}\}$.

(1) Center-of-mass coordinates should be expressed by $\{\boldsymbol{W}\}$ in the usual way by the use of physical coordinates,

$$\langle\sum_{i=1}^{A}\boldsymbol{a}_i\rangle=\sum_{i=1}^{A}\boldsymbol{Z}_i=\sum_{i=1}^{A}\boldsymbol{W}_i\,. \tag{3·2}$$

(2) Angular momentum and number of oscillator quanta and other generators of Elliott $SU(3)$ group should be expressed by $\{\boldsymbol{W}\}$ in the usual way by the use of physical coordinates,

$$\langle\sum_{i=1}^{A}a_{i\sigma}^{\dagger}a_{i\tau}\rangle=\sum_{i=1}^{A}\sum_{j=1}^{A}Z_{i\sigma}^{*}Q_{ij}Z_{j\tau}=\sum_{i=1}^{A}W_{i\sigma}^{*}W_{i\tau}\,, \tag{3·3}$$

where $\sigma, \tau=x, y, z$ and

$$Q_{ij}=B_{ij}B_{ji}^{-1}=\frac{\partial}{\partial(\boldsymbol{Z}_i^{*}\cdot\boldsymbol{Z}_j)}\log\langle\Phi(\boldsymbol{Z})|\Phi(\boldsymbol{Z})\rangle \tag{3·4}$$

is a hermitian matrix.

(3) The definition of $\{\boldsymbol{W}\}$ should be independent of the choice of the origin of phase space, i.e., $\boldsymbol{Z}_i\to\boldsymbol{Z}_i+\boldsymbol{c}$ should result in $\boldsymbol{W}_i\to\boldsymbol{W}_i+\boldsymbol{c}$, where $\boldsymbol{c}$ is an arbitrary constant vector.

(4) The definition of $\{\boldsymbol{W}\}$ should be independent of the choice of the direction of

phase space, i.e., $\boldsymbol{Z}_i \to R\boldsymbol{Z}_i$ should result in $\boldsymbol{W}_i \to R\boldsymbol{W}_i$, where R is an arbitrary rotation matrix.

(5) When antisymmetrization effect is weak, $\{\boldsymbol{W}\}$ should coincide with $\{\boldsymbol{Z}\}$.

Taking into account these requirements, we define $\{\boldsymbol{W}\}$ as

$$\boldsymbol{W}_i = \sum_{j=1}^{A} (\sqrt{Q})_{ij} \boldsymbol{Z}_j \,. \tag{3·5}$$

Note that Q depends on $\{\boldsymbol{Z}\}$. Although square root of Q has arbitrariness of unitary transformation, we choose the following convention,

$$Q = UDU^{\dagger}\,, \quad \sqrt{Q} = U\sqrt{D}\,U^{\dagger}\,, \tag{3·6}$$

where U is the diagonalizing unitary matrix of Q and D is the diagonal matrix. Since Q is positive definite, there is no arbitrariness in this definition.

The requirement (2) is manifestly satisfied by this definition. Since Q is rotationally invariant, the requirement (4) is also satisfied. If all $\boldsymbol{Z}_i$ are far away from one another so that (normalized) overlaps between different single particle states are negligible, then $Q_{ij} \to \delta_{ij}$. Hence the requirement (5) is satisfied. In order to prove that the requirements (1) and (3) are satisfied, we introduce eigencoordinates $\{\boldsymbol{Z}'\}$ and $\{\boldsymbol{W}'\}$ as

$$\boldsymbol{Z}'_i = \sum_j U^*_{ji} \boldsymbol{Z}_j \,, \quad \boldsymbol{W}'_i = \sum_j U^*_{ji} \boldsymbol{W}_j \,. \tag{3·7}$$

If we denote eigenvalues of Q as $\lambda_1, \lambda_2, \cdots, \lambda_A$, Eq. (3·5) can be rewritten as

$$\boldsymbol{W}'_i = \sqrt{\lambda_i}\, \boldsymbol{Z}'_i \,. \tag{3·8}$$

The equation

$$\sum_{j=1}^{A} Q_{ij} = \sum_{j=1}^{A} B_{ij} B^{-1}_{ji} = 1 \tag{3·9}$$

indicates that Q has an eigenvector $(1, 1, \cdots, 1)^T$ for the eigenvalue 1. We define this eigenvalue and eigenvector as the first ones, namely,

$$\lambda_1 = 1 \,, \tag{3·10}$$

$$U_{i1} = 1/\sqrt{A} \quad \text{for } i = 1, 2, \cdots, A \,. \tag{3·11}$$

Then it follows that

$$\sum_i \boldsymbol{W}_i = \sqrt{A}\, \boldsymbol{W}'_1 = \sqrt{A}\, \boldsymbol{Z}'_1 = \sum_i \boldsymbol{Z}_i \,, \tag{3·12}$$

which means that the requirement (1) is satisfied. Under Galilei transformation $\boldsymbol{Z}_i \to \boldsymbol{Z}_i + \boldsymbol{c}$, Q does not change as we have proved in § 2. Hence U and λ are also Galilei invariant. The changes of $\boldsymbol{Z}'_i$ are therefore

$$\boldsymbol{Z}'_i \to \sum_j U^*_{ji} (\boldsymbol{Z}_j + \boldsymbol{c}) = \boldsymbol{Z}'_i + \sum_j U_{j1} U^*_{ji} \sqrt{A}\, \boldsymbol{c} = \boldsymbol{Z}'_i + \delta_{i1} \sqrt{A}\, \boldsymbol{c} \,. \tag{3·13}$$

The last equation is due to the unitarity of U. This equation means that only the

center-of-mass coordinate changes by Galilei transformation and other relative coordinates $\boldsymbol{Z}_2', \cdots, \boldsymbol{Z}_A'$ do not change. Since λ_i are invariant under Galilei transformation, due to Eq. (3·8) the changes of $\boldsymbol{W}_i'$ are also

$$\boldsymbol{W}_i' \to \boldsymbol{W}_i' + \delta_{i1}\sqrt{A}\,\boldsymbol{c}\,, \tag{3·14}$$

which means

$$\boldsymbol{W}_i \to \boldsymbol{W}_i + \boldsymbol{c}\,. \tag{3·15}$$

Thus the requirement (3) is proved to be satisfied.

In the case of two nucleons of the same spin and isospin, the relative coordinate is written as

$$\boldsymbol{w} = \sqrt{\frac{\partial \log\langle \Phi|\Phi\rangle}{\partial(\boldsymbol{z}^*\cdot\boldsymbol{z})}}\,\boldsymbol{z} = \sqrt{\frac{1+\exp(-\boldsymbol{z}^*\cdot\boldsymbol{z})}{1-\exp(-\boldsymbol{z}^*\cdot\boldsymbol{z})}}\,\boldsymbol{z}\,, \tag{3·16}$$

$$\boldsymbol{z} \equiv \boldsymbol{Z}_2' = \frac{1}{\sqrt{2}}(\boldsymbol{Z}_1 - \boldsymbol{Z}_2)\,, \quad \boldsymbol{w} \equiv \boldsymbol{W}_2' = \frac{1}{\sqrt{2}}(\boldsymbol{W}_1 - \boldsymbol{W}_2)\,. \tag{3·17}$$

This is identical to the application to the two-nucleon system of the canonical coordinate derived by Saraceno, Kramer and Fernandez[22] in time-dependent cluster model. Our physical coordinate $\{\boldsymbol{W}\}$ is introduced on the basis of their theory aiming at an extension to general many-body (or -cluster) system. Although $\{\boldsymbol{W}\}$ is no more exact canonical coordinate if $A \geq 3$, it can be regarded as physical coordinate as discussed above.

3.2. *Pauli forbidden region*

In AMD, we treat fermionic nature of nucleons exactly, because the wave function of A-body system is represented by a Slater determinant. Pauli principle has therefore been fully incorporated in our model wave function, in contrast to QMD. In this subsection, we will study how Pauli principle appears in the physical coordinates $\{\boldsymbol{W}\}$. On the basis of this study, we will discuss in the next subsection the Pauli blocking in two-nucleon collisions. For simplicity of notation, we consider the case where all nucleons have the same spin and isospin.

From Eq. (3·3) the number of harmonic oscillator quanta $N_{\rm osc}$ can be written by $\{\boldsymbol{W}\}$ as

$$N_{\rm osc} = \sum_{i=1}^{A} \boldsymbol{W}_i^* \cdot \boldsymbol{W}_i = \frac{1}{A}\sum_{i<j} |\boldsymbol{W}_i - \boldsymbol{W}_j|^2\,, \tag{3·18}$$

where we have assumed that the center-of-mass is at the origin, $\sum_i \boldsymbol{W}_i = 0$. For the case $A=2$, the configuration which minimizes $N_{\rm osc}$ is $(0s)^1(0p)^1$ and the minimum value of $N_{\rm osc}$ is therefore 1. From (3·18), it follows that $\boldsymbol{W}_1$ and $\boldsymbol{W}_2$ cannot get closer than $\sqrt{2}$ however small $|\boldsymbol{Z}_1 - \boldsymbol{Z}_2|$ may be. In fact, according to the theory of Saraceno et al.,[22] our physical coordinates $\{\boldsymbol{W}\}$ are exact canonical coordinates in the case $A=2$, and the region $|\boldsymbol{W}_1 - \boldsymbol{W}_2| < \sqrt{2}$ is called Pauli forbidden region. For such Pauli forbidden $\{\boldsymbol{W}\}$ there is no corresponding $\{\boldsymbol{Z}\}$ which satisfies Eq. (3·5). If $\{\boldsymbol{W}\}$ is out of Pauli forbidden region, i.e., it is Pauli allowed, such a corresponding $\{\boldsymbol{Z}\}$ is obtained by

solving nonlinear equation (3·5) or (3·16).

For the case $A \geq 3$, we also call those $\{\boldsymbol{W}\}$ which have no corresponding $\{\boldsymbol{Z}\}$ to be Pauli forbidden and others Pauli allowed. Although these are the definitions of Pauli forbidden and Pauli allowed $\{\boldsymbol{W}\}$, we would like to have such an intuitive picture as for the case $A=2$, in identifying the Pauli forbidden and Pauli allowed $\{\boldsymbol{W}\}$. Unfortunately the condition

$$(N_{\mathrm{osc}})_{\min} \leq \frac{1}{A}\sum_{i<j}|\boldsymbol{W}_i - \boldsymbol{W}_j|^2 \tag{3·19}$$

is a necessary condition but not a sufficient condition for $\{\boldsymbol{W}\}$ to be Pauli allowed. However it is to be noted from Eq. (3·19) that the average of $|\boldsymbol{W}_i - \boldsymbol{W}_j|^2$ is greater than 2, namely,

$$\sqrt{\langle|\boldsymbol{W}_i - \boldsymbol{W}_j|^2\rangle} = \sqrt{\frac{2(N_{\mathrm{osc}})_{\min}}{A-1}} \geq \sqrt{2} \tag{3·20}$$

for any A. Furthermore we have found interesting facts for the cases $A=3, 4$. When all $\boldsymbol{Z}_i$ are very close to 0, $\boldsymbol{W}_i$ always form a regular triangle for $A=3$ or a regular tetrahedron for $A=4$ in the six-dimensional phase space. The length of sides of the triangle or the tetrahedron is always $\sqrt{2}$. The direction of the triangle or the tetrahedron in phase space, of course, depends on $\boldsymbol{Z}_i$, but $\boldsymbol{Z}_i$ are arbitrary as long as they are very small. These facts, together with many numerical experiments, suggest that it is reasonable to assume that the distance between any two $\boldsymbol{W}_i$ cannot be too small in order that $\{\boldsymbol{W}\}$ may be Pauli allowed, though the minimum value might not be $\sqrt{2}$ for general A.

3.3. *Details of two-nucleon collisions*

The physical coordinates $\boldsymbol{R}_i$ and $\boldsymbol{P}_i$ which are the real and imaginary parts of $\boldsymbol{W}_i$ are used in two-nucleon collision processes. Two nucleons i and j are made to scatter with the impact parameter dependent probability $P(b)$ which is proportional to the density overlap of two Gaussian wave packets,

$$P(b) = \frac{\nu\sigma_{\mathrm{NN}}}{\pi} e^{-\nu b^2}, \tag{3·21}$$

when the distance of these two nucleons gets minimum between two time steps $t-\Delta t$ and t, i.e.,

$$f(\alpha) = |(1-\alpha)\boldsymbol{R}_{\mathrm{rel}}(t-\Delta t) + \alpha \boldsymbol{R}_{\mathrm{rel}}(t)| \tag{3·22}$$

takes its minimum value for α between 0 and 1. The impact parameter b is this minimum value of $f(\alpha)$. We use the energy dependent cross section

$$\sigma_{\mathrm{NN}} = \frac{\sigma_0}{1+E_{\mathrm{NN}}/E_0}, \quad \sigma_0 = 100\ \mathrm{mb}, \quad E_0 = 200\ \mathrm{MeV}, \tag{3·23}$$

where $E_{\mathrm{NN}} = M\dot{\boldsymbol{R}}_{\mathrm{rel}}^2/2$. This choice of cross section ensures that collision probability defined by (3·21) is smaller than 1 when we take $\nu = 0.16\ \mathrm{fm}^{-2}$.

By the collision, the positions $\boldsymbol{R}_i$ and $\boldsymbol{R}_j$ are not changed and momenta $\boldsymbol{P}_i$ and $\boldsymbol{P}_j$

are changed stochastically into $\boldsymbol{P}_i'$ and $\boldsymbol{P}_j'$,

$$\begin{aligned}\boldsymbol{P}_i' &= \frac{1}{2}\boldsymbol{P}_{\rm cm} + P_{\rm rel}'\hat{\boldsymbol{n}}\,,\\ \boldsymbol{P}_j' &= \frac{1}{2}\boldsymbol{P}_{\rm cm} - P_{\rm rel}'\hat{\boldsymbol{n}}\,,\end{aligned} \tag{3·24}$$

where $\boldsymbol{P}_{\rm cm}=\boldsymbol{P}_i+\boldsymbol{P}_j$ and $\hat{\boldsymbol{n}}$ is a randomly chosen unit vector. $P_{\rm rel}'$ is the relative momentum of final state which is at first taken to be equal to the initial relative momentum $|\boldsymbol{P}_i-\boldsymbol{P}_j|/2$. Then we calculate $\{\boldsymbol{Z}'\}$ which corresponds to $\{\boldsymbol{W}'\}$ by solving the nonlinear equation (3·5) selfconsistently. When the inverse transformation from $\{\boldsymbol{W}'\}$ to $\{\boldsymbol{Z}'\}$ does not exist, the collision is considered to be Pauli blocked as explained in the previous subsection. But since executing the inverse transformation of (3·5) is not an easy numerical task, we would like to see through some Pauli forbidden $\{\boldsymbol{W}'\}$ without solving nonlinear equation. As we have seen in the previous subsection, it seems reasonable to assume that the distance between any two $\boldsymbol{W}'$ cannot be too small. In the practical calculation, therefore, the collision is judged to be Pauli blocked without solving (3·5), when there is another nucleon in any of two spheres of radius a centered at $\boldsymbol{W}_i'$ and $\boldsymbol{W}_j'$ respectively, where a must be less than $\sqrt{2}$. The smaller a is, the more exact this prescription is, but the harder the numerical calculation is. We take $a=1.348$ in the calculation reported in this paper. The possibility that Pauli allowed $\{\boldsymbol{W}\}$ is misjudged as Pauli forbidden by this prescription is expected to be small. When all $|\boldsymbol{W}_k-\boldsymbol{W}_i|$ and $|\boldsymbol{W}_l-\boldsymbol{W}_j|$ $(k\neq i,\ l\neq j)$ are greater than a, we try to solve Eq. (3·5) selfconsistently. The collision is Pauli blocked if no solution is found, and it is not Pauli blocked at this stage if a solution is found.

If the collision is not Pauli blocked, we calculate the energy E' for the final state $\{\boldsymbol{Z}'\}$. There is, of course, no reason why E' should coincide with the initial energy E. We must therefore modify the final relative momentum $P_{\rm rel}'$ in (3·24) so that the energy conservation becomes better. The modified relative momentum $P_{\rm rel}''$ is determined by

$$\frac{P_{\rm rel}''^{\,2}}{M}-\frac{P_{\rm rel}'^{\,2}}{M}=E-E'\,. \tag{3·25}$$

This modification would give the exact energy conservation if the total energy were the sum of naive kinetic energy and potential energy which depends only on $\boldsymbol{R}$. The modified $\boldsymbol{W}''$ are given by

$$\begin{aligned}\boldsymbol{P}_i'' &= \frac{1}{2}\boldsymbol{P}_{\rm cm} + P_{\rm rel}''\hat{\boldsymbol{n}}\,,\\ \boldsymbol{P}_j'' &= \frac{1}{2}\boldsymbol{P}_{\rm cm} - P_{\rm rel}''\hat{\boldsymbol{n}}\,.\end{aligned} \tag{3·26}$$

After this modification, we calculate $\{\boldsymbol{Z}''\}$ corresponding to $\{\boldsymbol{W}''\}$, and then modify again $\{\boldsymbol{W}''\}$ into $\{\boldsymbol{W}'''\}$ in the same way so that the energy conservation becomes better. We repeat this procedure until the energy conservation is achieved within the accuracy of 2 MeV. When the inverse transformation does not exist in the course of this procedure of energy correction, the collision is judged to be Pauli blocked. In many cases one or two correction steps are sufficient to achieve the energy conservation.

When energy conservation is not achieved after 4 correction steps, the collision is regarded as not taking place. But such bad events occur only once in more than 10 simulations.

§ 4. Application to the study of fragment mass distribution

4.1. *Fragment mass distribution and shell effect*

We have applied the AMD with two-nucleon collisions to the reaction $^{12}C+^{12}C$ with incident energy $E_{lab}/A=28.7$ MeV. Since this incident energy is comparable to the Fermi energy of nuclei, the effect of antisymmetrization may play important roles not only in the ground state properties of initial nuclei but also in the dynamics of the reaction. The effective two-nucleon force and other parameters used in this calculation are the same as those given in §§ 2 and 3. We have executed about 1000 simulations with the impact parameters ranging over $0\text{ fm}<b<7\text{ fm}$, using FACOM VP-2600 at Data Processing Center, Kyoto University, for about 9 hours. In each simulation the time development of the system has been traced until $t=200\text{ fm}/c$ after the contact of two nuclei, which seems sufficient for the investigation of dynamical reaction process. The violation of the energy conservation in solving the equation of motion has turned out to be about 0.1 MeV, while that due to the energy correction prescription in two-nucleon collisions is 2 MeV as explained in the previous section.

In Fig. 3, an example of the time development of the density and the physical coordinates, which are projected onto the reaction plane, is displayed. In the initial state of this reaction, two oblately-deformed ^{12}C nuclei with randomly chosen directions are boosted toward each other with impact parameter $b=3.2$ fm. An alpha cluster is picked out from the projectile (moving from left to right) by the target and only a neutron of this alpha cluster is transferred to the target, leaving a ^{3}He fragment. The projectile-like ^{8}Be fragment has broken up into two alpha particles before $t=200\text{ fm}/c$. The density shown in this figure is of course calculated from the AMD wave function. We can see that the physical positions, which are represented by crosses in Fig. 3, are consistent with the density.

In Fig. 4 the mass distribution of fragments is shown, and in Fig. 5 the isotope distributions from He to N are compared with the experimental data by Czudek et al.[25] The fragments with mass number 12 are not shown because it is difficult in

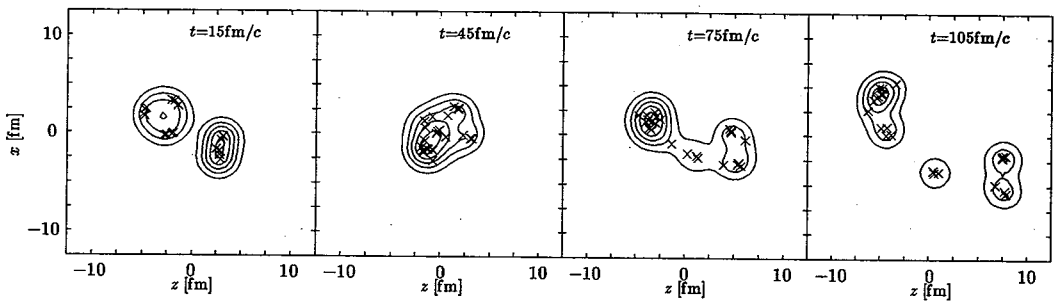

Fig. 3. Time development of density and physical coordinates projected onto the reaction plane.

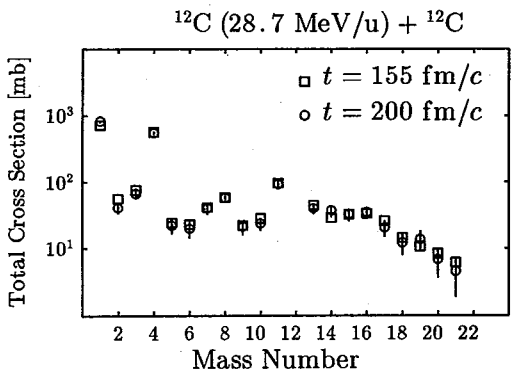

Fig. 4. Mass distribution for the reaction ^{12}C(28.7 MeV/u)+^{12}C. Circles with error bars are the cross sections at t=200 fm/c and boxes at t =155 fm/c after the first contact of two nuclei.

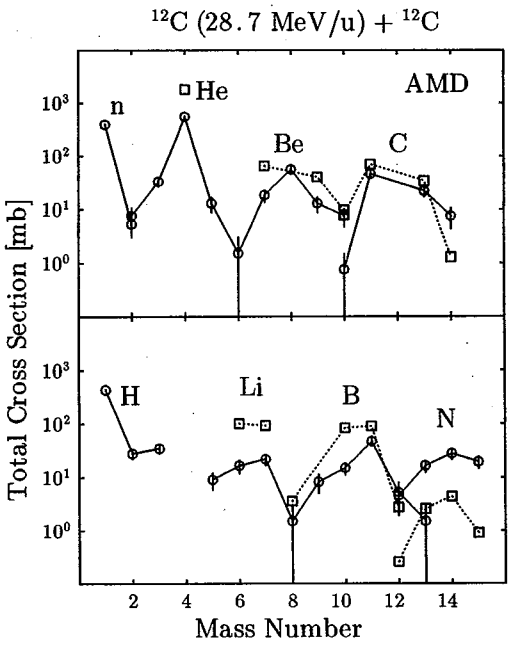

Fig. 5. Isotope distribution for the reaction ^{12}C (28.7 MeV/u)+^{12}C. Circles with error bars are the results of AMD calculation and boxes experimental values. Lines connect isotopes.

AMD calculation to distinguish scattered ^{12}C from unscattered ^{12}C. Only those fragments which have momenta $p_F/A_F > 100$ MeV/c and emission angles $4° < \theta_F < 36°$ in the laboratory system are taken into account. This selection of emission angles is the same as the experimental situation while the selection of momenta approximately corresponds to it. The quantitative feature of mass distribution does not depend on the detail of this selection of momenta so much.

It should be noted that we are now comparing the experimental result with the result of AMD calculation which has been truncated at t=200 fm/c. From Fig. 4, it can be understood that mass distribution has become almost stationary by this time because the mass distribution at t=155 fm/c and that at t=200 fm/c are almost identical. There is, however, the possibility that the mass distribution changes after t=200 fm/c until fragments reach the detector. It must be kept in mind that what we have calculated is the result of dynamical reaction and does not fully include statistical decay process of long time scale.

We notice the appearance of shell effect or α-clustering effect, i.e., the enhancement of the cross sections of α and ^{8}Be. The enhancement of alpha particles of experimental data is reproduced qualitatively, though it is still underestimated. Since ^{8}Be is unstable, it is expected to decay into lighter fragment, such as ^{7}Li, ^{6}Li and ^{7}Be, as well as into 2α after t=200 fm/c. As for the fragments with mass number $A>12$, the shell effect has not appeared in mass distribution, which is understood because those fragments are expected to be in highly excited states.

It should be noted that the appearance of shell effect, or α-clustering effect, is not a trivial result of our model. As the initial state we have used not the clustering state but the shell model state which has been obtained by frictional cooling method as explained in § 2.3. Although the shell model state also has [4]-symmetry, two-nucleon

collision process has the effect to break this symmetry of the wave function or $\{\boldsymbol{Z}\}$.

Intermediate mass fragments, which we call here the fragments with mass number $6 \leq A \leq 9$, are underestimated. The ratio of calculated cross section to the observed one is between 20 % and 30 % for each of nuclei which are stable and hence observed in experiment. (^{9}B and ^{8}Be are not observed because they can decay to p $+2\alpha$ and to 2α respectively even though they are in the ground states.) This tendency of underestimation is consistent with the result of QMD calculation,[26] apart from the enhancement of ^{8}Be.

The cross sections of fragments with $A=11$ are well reproduced. It is very reasonable that ^{11}C and ^{11}B are produced with the nearly equal cross sections, because a proton and a neutron should be stripped with the same probability as long as Coulomb interaction is not important. For the same reason, ^{13}C and ^{13}N are produced with the same probability in AMD calculation, while large difference of cross sections of these fragments is observed in experiment. Such difference cannot appear at least in the dynamical process because it is difficult to expect that Coulomb interaction plays an important role.

4.2. *Preliminary study of the statistical decay yield*

In the previous subsection, we discussed the mass distribution which is the result of dynamical process before $t=200$ fm/c, by which the thermalization of fragments are expected to have been achieved. The mass distribution, however, will change after $t=200$ fm/c due to the statistical cascade decays. In Fig. 6, we show the internal energies of fragments which have been obtained by AMD calculation. It can be seen that many fragments are excited enough to decay into lighter fragments by evaporating particles. It is therefore indispensable to study statistical cascade decays in order to understand the experimentally observed mass distribution.

We have estimated the statistical decay yield by a cascade calculation. We used the code written by one of the authors (T.M.) which is a modified version of the code CASCADE of Pühlhofer.[27] Let us briefly summarize the formulation used in our code

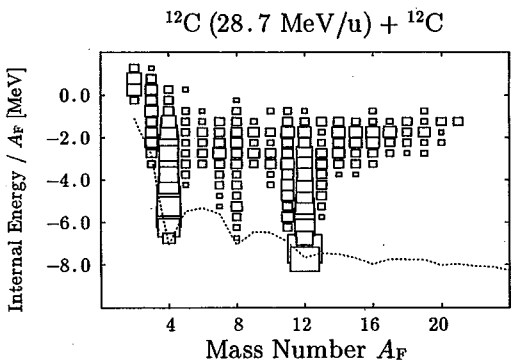

Fig. 6. Internal energies per nucleon of fragments which are produced by AMD calculation. The length of side of each rectangle is proportional to (the yield)$^{1/3}$. Dotted line represents the minimum binding energies of the isobars.

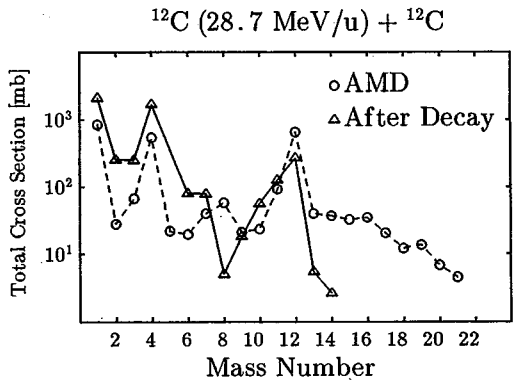

Fig. 7. Comparison of the mass distributions before and after the statistical cascade decays for the reaction ^{12}C(28.7 MeV/u)+^{12}C.

which is essentially the same as that of Ref. 27). By the consideration of detailed balance, we can evaluate the partial width of the decay from a nucleus 1 with excitation energy and spin (E_1, J_1) into two nuclei 2 and 3 with (E_2, J_2) and (E_3, J_3) respectively as

$$\Gamma dE_2 dE_3 = \frac{\rho_2(E_2, J_2)\rho_3(E_3, J_3)}{2\pi\rho_1(E_1, J_1)} \sum_{J_{23}=|J_2-J_3|}^{J_2+J_3} \sum_{L=|J_1-J_{23}|}^{J_1+J_{23}} T_L dE_2 dE_3 , \qquad (4\cdot1)$$

where ρ_i, $i=1, 2, 3$, is the level density of each nucleus and T_L is the transmission coefficient of the partial wave L in the fusion reaction $2+3\rightarrow1$ with the incident energy which depends on E_1, E_2, E_3 and the Q-value. Note that the lighter fragment (nucleus 3) as well as heavier fragment (nucleus 2) can be in the excited state in this formulation. In the excitation energy range where experimentally observed individual levels are available, we treat them instead of the averaged level density. Otherwise we use the level density formula of Fermi gas model with the level density parameter $a=A/8\,\mathrm{MeV}^{-1}$. The pairing energy is taken into account. We have not taken into account parity and isospin quantum numbers to specify levels. The other ingredient, the transmission coefficient T_L, is determined by the assumption of strong absorption, i.e., $T_L=1$ if $L\leq L_c$ and $T_L=0$ otherwise, where L_c is the critical angular momentum for the fusion reaction $2+3\rightarrow1$.

Starting with the result of AMD calculation at $t=200\,\mathrm{fm}/c$, we have calculated the statistical cascade decays, which have changed the mass distribution as shown in Fig. 7. In Fig. 8, the final isotope distribution is compared with the experimental data. We can see the reproduction of the experimental data has become better for all isotopes except for ^{13}C and ^{14}C. Especially the enhancement of alpha particles is reproduced quantitatively and the production cross sections of all intermediate mass fragments are reproduced within a factor 2.

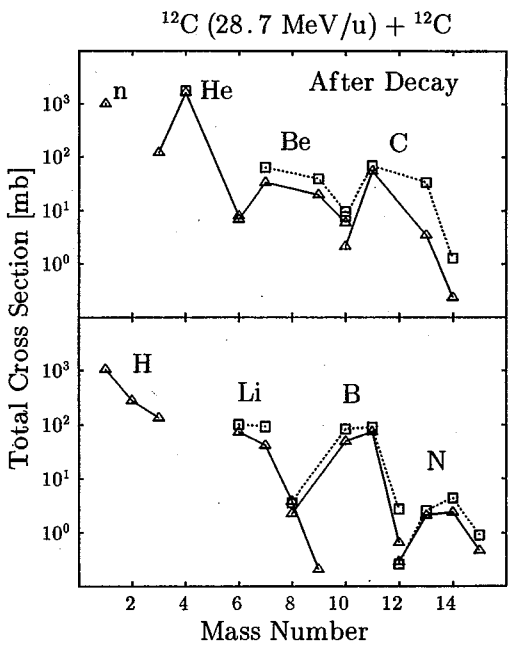

Fig. 8. Isotope distribution for the reaction ^{12}C (28.7 MeV/u)+^{12}C after the statistical cascade decays. Triangles are the results of the cascade calculation and boxes experimental values. Lines connect isotopes.

In this calculation, we have restricted the lighter daughter nucleus in its ground state at each cascade step, i.e., we have assumed $\rho_3(E_3)=\delta(E_3)$ in Eq. (4·1). We have also made calculation with looser restriction $E_3<7.5$ MeV but we have obtained almost the same result as that of the above assumption, which justifies the assumption that the evaporation of excited fragments are not so important.

In Fig. 9, we show which fragments at the end of AMD calculation have contributed to the production cross section of each mass number after statisti-

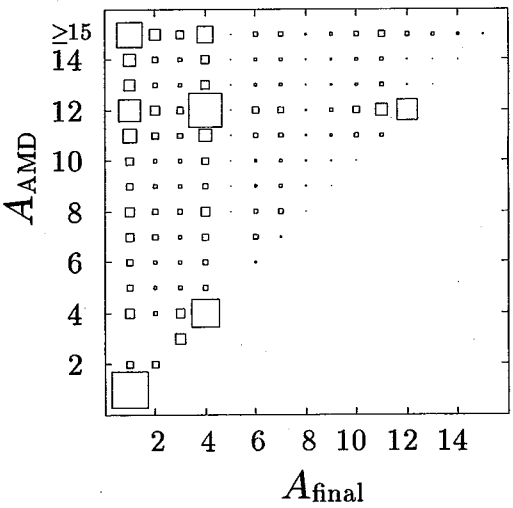

Fig. 9. The diagram which represents contributions of fragments obtained by AMD calculation to the final mass distribution. The vertical axis is the mass number A_{AMD} of fragments produced by AMD calculation, and the horizontal axis is the mass number A_{final} of final products after statistical cascade decays. The area of each box is proportional to the yield with which the fragments with A_{AMD} have decayed into the fragments with A_{final}.

cal cascade decays. It can be seen that the shortage of alpha particle yield in AMD calculation is filled mainly by statistical decay of ^{12}C. This means that about one third of observed alpha particles are produced in the dynamical reaction stage, while the others are produced by sequential statistical decays mainly of excited projectile and target nuclei. As for the final fragments with mass number $A=10$, 11, the main contribution is also made by decays of ^{12}C. The intermediate mass fragments have various origins including large contribution from excited ^{12}C. Although the experimental data of the cross sections of fragments with $A\leq 3$ are not available, our calculation suggests that about 40 % of nucleons are produced in the dynamical stage of the reaction and the others are evaporated from fragments in the statistical cascade decays. We can also see that most of deuterons and tritons are produced in the statistical cascade decays.

Our calculation, AMD plus statistical decay, has underestimated the production cross sections of most kinds of fragments by factors between 1 and 2. Some part of this discrepancy may be due to the difference between the selection of fragments in our calculation and the experimental situation. Furthermore our model has a free parameter, namely the cross section of two-nucleon collisions. If we had taken larger one than Eq. (3·23), we would have obtained larger cross sections as the final result.

§ 5. Summary and discussion

In this paper, we have formulated the two-nucleon collisions in antisymmetrized version of molecular dynamics, which has established a new microscopic simulation framework for heavy ion reactions. We have named this new framework simply AMD.

AMD has been proved to be able to describe the ground state as well as Hartree-Fock theory is. Hence in AMD we can start simulations with initial states expressed in the form of wave functions of good quality, which is a feature of AMD superior to any other tractable simulation frameworks.

The binding energies of nuclei especially lighter than the ^{12}C nucleus have been shown to be reproduced excellently. Furthermore we have proposed a prescription for the subtraction of spurious zero-point energy of fragment center-of-mass motion.

These two things have made it possible to reproduce the threshold energies of fragmentation of the projectile into all pairs of fragments in the reaction $^{12}C+^{12}C$, which we have studied in order to verify the usefulness of the AMD.

AMD without two-nucleon collisions is interpreted as an approximation of time-dependent Hartree-Fock (TDHF) theory, because AMD parametrizes the single particle wave functions of TDHF by a finite number of parameters $\{\boldsymbol{Z}\}$. In order to improve AMD, we can generalize the single particle wave functions of AMD. For example, we can treat the width parameter ν of each nucleon i as time dependent complex variable $\nu_i(t)$, as the original FMD of Feldmeier[13] does. This new degree of freedom seems important at least in low incident energy region where two-nucleon collisions are suppressed by Pauli blocking, as has been suggested by Bauhoff et al.[21] in the study of low energy fusion reactions with the use of TDCM. In the case of the QMD approach, there has been reported recently a work[18] which uses time-dependent width parameters $\nu_i(t)$. Another generalization is to treat spin wave functions as time-dependent,[13] which will, however, make the calculation of Hamiltonian at least four times as hard because the block-diagonality of $B_{ij}=\langle\varphi_i|\varphi_j\rangle$ will be half lost.

When the time variation of $\nu_i(t)$ is taken into account, the problem of the spurious zero-point kinetic energy for nucleon emission is expected to be treated better, because the width parameter $\nu(t)$ can become small so as to make the zero-point energy $3\hbar^2\nu(t)/2M$ small. However one cannot necessarily expect sufficient amount of the change of $\nu(t)$ parameter during the nucleon emission process and furthermore in the case of cluster emission the time variation of $\nu_i(t)$ will not be helpful for the spurious zero-point energy problem.

In view of the present situation that we have no efficient method to avoid the spurious zero-point kinetic energy of fragment center-of-mass motion, a new prescription which we proposed in this paper for the solution of this problem is very useful in spite of its somewhat artificial character.

Two-nucleon collision process has been incorporated into AMD in the same way as in QMD by introducing the physical coordinates $\{\boldsymbol{W}\}$. The Pauli forbidden region which appears in the space of $\{\boldsymbol{W}\}$ plays an essential role in the Pauli blocking of two-nucleon collisions. It should be noted that AMD is different from extended TDHF or VUU (Vlasov-Uehling-Uhlenbeck) approach, with respect to the two-nucleon collisions. AMD, as well as QMD, tries to describe not only one-body observables but also N-body observables, and two-nucleon collisions should be interpreted not as the effects of higher order correlations on the one-body density matrix but as jumps from an N-body wave function to another N-body wave function.

In order to demonstrate the ability of AMD, we have applied it to the study of the fragment formation in the reaction $^{12}C+^{12}C$ at incident energy $E_{lab}/A=28.7$ MeV. As the result of proper treatment of antisymmetrization, the shell effect or the alpha-clustering effect observed in mass distribution is reproduced qualitatively by the AMD calculation. Furthermore we have succeeded in quantitative reproduction of mass distribution by taking account of statistical cascade decays of excited fragments. We have pointed out that there are two components of alpha particles; the first is the dynamically created alpha particles and the second is the products of statistical cascade decays of heavier fragments. The former yield is about one third of the total

alpha yield. In the model of QMD plus statistical cascade decay, the first component does not appear and the shell effect appears only after the statistical cascade decays in which the shell effect in binding energy is taken into account. On the other hand, if TDCM is used to analyze this reaction, most of observed alpha particle cross section will be reproduced only by the dynamical process because the degrees of freedom of alpha-cluster excitation are not described in TDCM and too much energy will be given to the degrees of freedom of relative motion among alpha clusters. Thus AMD is a simulation method which does not assume any clusters but can describe the shell effects and the clustering effects in the case when they should appear.

We have compared our AMD calculation of fragment mass distribution with the QMD calculation[26] and have found that the main feature of the calculated results is common between the two, except that the shell effect in the dynamical process is not describable in QMD. We will discuss this comparison in more detail in the forthcoming paper of ours.[26]

In this application, we have used the Volkov force as the effective interaction. Although this force has been widely used in the study of nuclear structure and low energy reactions, it does not have a density-dependent component. We, however, think that the use of this force in our present study is justified since at our present incident energy, 28.7 MeV/nucleon, the density does not become so high. When we study reactions at much higher incident energy, we need to modify this effective force so as to include a density-dependent term as was done in Ref. 28).

As has been discussed in this paper, AMD has been verified to be an excellent simulation framework for heavy ion reactions at least for the reproduction of fragment nuclide distribution, but at the same time it is an expensive one if one wants to apply it to heavier systems with mass number $A=A_P+A_T>50$, for example. This is because we must calculate $A^4/16$ terms for the evaluation of the gradients of Hamiltonian. The reduction factor 16 is due to the block-diagonality of $B_{ij}=\langle\varphi_i|\varphi_j\rangle$. Further reduction may be possible if one uses the fact that B_{ij} is divided into smaller matrices when $\{\boldsymbol{Z}\}$ are divided into some groups which are separated from one another in phase space. Another approximation may be possible if one is interested in the fragmentation of relatively light projectile on the heavy target. In such reactions, the target can be treated approximately as an external mean field and a group of scatterers for the projectile nucleons as proposed in Ref. 11).

References

1) J. Aichelin and H. Stöcker, Phys. Lett. **B176** (1986), 14.
J. Aichelin, Phys. Rep. **202** (1991), 233.
2) G. Peilert, H. Stöcker, W. Greiner, A. Rosenhauer, A. Bohnet and J. Aichelin, Phys. Rev. **C39** (1989), 1402.
3) A. Bohnet, N. Ohtsuka, J. Aichelin, R. Linden and A. Faessler, Nucl. Phys. **A494** (1989), 34.
4) T. Maruyama, A. Ohnishi and H. Horiuchi, Phys. Rev. **C42** (1990), 386.
5) C. Y. Wong, Phys. Rev. **C25** (1982), 1460.
6) G. F. Bertsch and S. Das Gupta, Phys. Rep. **160** (1988), 189.
7) W. Cassing, V. Metag, U. Mosel and K. Niita, Phys. Rep. **188** (1990), 363.
8) C. Gregoire, B. Remaud, F. Sebille, L. Vinet and Y. Raffray, Nucl. Phys. **A465** (1987), 317.
9) A. Ohnishi, H. Horiuchi and T. Wada, Phys. Rev. **C41** (1990), 2147.
10) C. Hartnack, Li Zhuxia, L. Neise, G. Peilert, A. Rosenhauer, H. Sorge, J. Aichelin, H. Stöcker and W. Greiner, Nucl. Phys. **A495** (1989), 303c.

11) A. Ohnishi, T. Maruyama and H. Horiuchi, Prog. Theor. Phys. **87** (1992), 417.
12) D. H. Boal and J. N. Glosli, Phys. Rev. **C38** (1988), 2621.
D. H. Boal, J. N. Glosli and C. Wicentowich, Phys. Rev. **C40** (1989), 601.
13) H. Feldmeier, Nucl. Phys. **A515** (1990), 147.
14) For example, P. Kramer and M. Saraceno, *Lecture Notes in Physics* **140** (Springer, Berlin, 1981).
15) H. Horiuchi, Nucl. Phys. **A522** (1991), 257c.
H. Horiuchi, T. Maruyama, A. Ohnishi and S. Yamaguchi, Preprint, KUNS 1028, Kyoto University.
16) H. Horiuchi, T. Maruyama, A. Ohnishi and S. Yamaguchi, *Proc. Int. Conf. on Nuclear and Atomic Clusters, Turku, 1991* (Springer), to be published.
Proc. Int. Symp. on Structure and Reactions of Unstable Nuclei, Niigata, 1991, ed. K. Ikeda and Y. Suzuki (World Scientific), p. 108.
17) C. Coriandò, R. Parwani and H. Yamagishi, Nucl. Phys. **A522** (1991), 591.
18) P. Valta, J. Konopka, M. Berenguer, A. Bohnet, J. Jaenicke, S. Huber, C. Hartnack, G. Peilert, L. W. Neise, J. Aichelin, H. Stöcker and W. Greiner, *Proc. IV Int. Conf. on Nucleus-Nucleus Collisions, Kanazawa, 1991,* to be published.
19) L. Wilet, E. M. Henley, M. Kraft and A. D. MacKellar, Nucl. Phys. **A282** (1977), 341.
20) S. Drożdż, J. Okolowcz and M. Ploszajczak, Phys. Lett. **109B** (1982), 145.
E. Caurier, B. Grammaticos and T. Sami, Phys. Lett. **109B** (1982), 150.
21) W. Bauhoff, E. Caurier, B. Grammaticos and M. Ploszajczak, Phys. Rev. **C32** (1985), 1915.
22) M. Saraceno, P. Kramer and F. Fernandez, Nucl. Phys. **A405** (1983), 88.
23) T. Wada, S. Yamaguchi and H. Horiuchi, Phys. Rev. **C41** (1990), 160.
24) A. Volkov, Nucl. Phys. **75** (1965), 33.
25) J. Czudek, L. Jarczyk, B. Kamys, A. Magiera, R. Siudak, A. Strzałkowski, B. Styczen, J. Hebenstreit, W. Oelert, P. von Rossen, H. Seyfarth, A. Budzanowski and A. Szczurek, Phys. Rev. **C43** (1991), 1248.
26) T. Maruyama, A. Ono, A. Ohnishi and H. Horiuchi, Prog. Theor. Phys. **87** (1992), No. 6.
H. Horiuchi, A. Ohnishi and T. Maruyama, *Proc. VI Int. Conf. on Nuclear Reaction Mechanisms, Varenna, 1991,* ed. E. Gadioli (Ricerca Scientifica ed Educazione Permanente, Milano), p. 238.
27) F. Pühlhofer, Nucl. Phys. **A280** (1977), 267.
28) T. Ando, K. Ikeda and A. Tohsaki, Prog. Theor. Phys. **64** (1980), 1608.